

Lawrence Berkeley National Laboratory

LBL Publications

Title

Investigation of suspected gulls in the Jurassic limestone strata of the Cotswold Hills, Gloucestershire, England using electrical resistivity tomography

Permalink

<https://escholarship.org/uc/item/1f1320ww>

Authors

Barron, AJM
Uhlemann, S
Pook, GG
[et al.](#)

Publication Date

2016-09-01

DOI

10.1016/j.geomorph.2016.05.028

Peer reviewed

Investigation of suspected gulls in the Jurassic limestone strata of the Cotswold Hills, Gloucestershire, England using electrical resistivity tomography

Author links open overlay panel [A.J.M. Barron^a](#) [S. Uhlemann^{ab}](#) [G.G. Pook^c](#) [L. Oxby^a](#)

Show more

Highlights

-

- Dry linear hollows in the English Cotswolds investigated as possible gulls

-

- Underlying structures found to be vertical 80 metre-deep rubble-filled zones

-

- Electrical resistivity tomography confirmed as ideal to investigate cambering

Abstract

An electrical resistivity [tomography](#) survey has clearly indicated the presence of substantial vertical zones of contrasting material beneath a set of conspicuous linear surface hollows that cut across a spur forming part of the Cotswold Hills [escarpment](#) in Gloucestershire. These zones are compared with nearby quarry exposures and are inferred to be gulls – graben-like structures at least 80 m deep filled with collapsed blocks of [bedrock](#) with intervening air-filled spaces, lying within areas of relatively undisrupted gently dipping strata, and which under some circumstances would present a significant geohazard. Our results confirm the great potential of this non-invasive and rapid survey technique for investigating such phenomena, and provide an exemplar for comparison with surveys elsewhere, to assist identification of similar features.

- [Previous article](#)
- [Next article](#)

Keywords

Cambering

Gull

Electrical resistivity tomography

Cotswold Hills

Geospatial data





**British
Geological Survey**

NATURAL ENVIRONMENT RESEARCH COUNCIL



Map data ©2018 Google
[Terms of Use](#)

MapSatellite

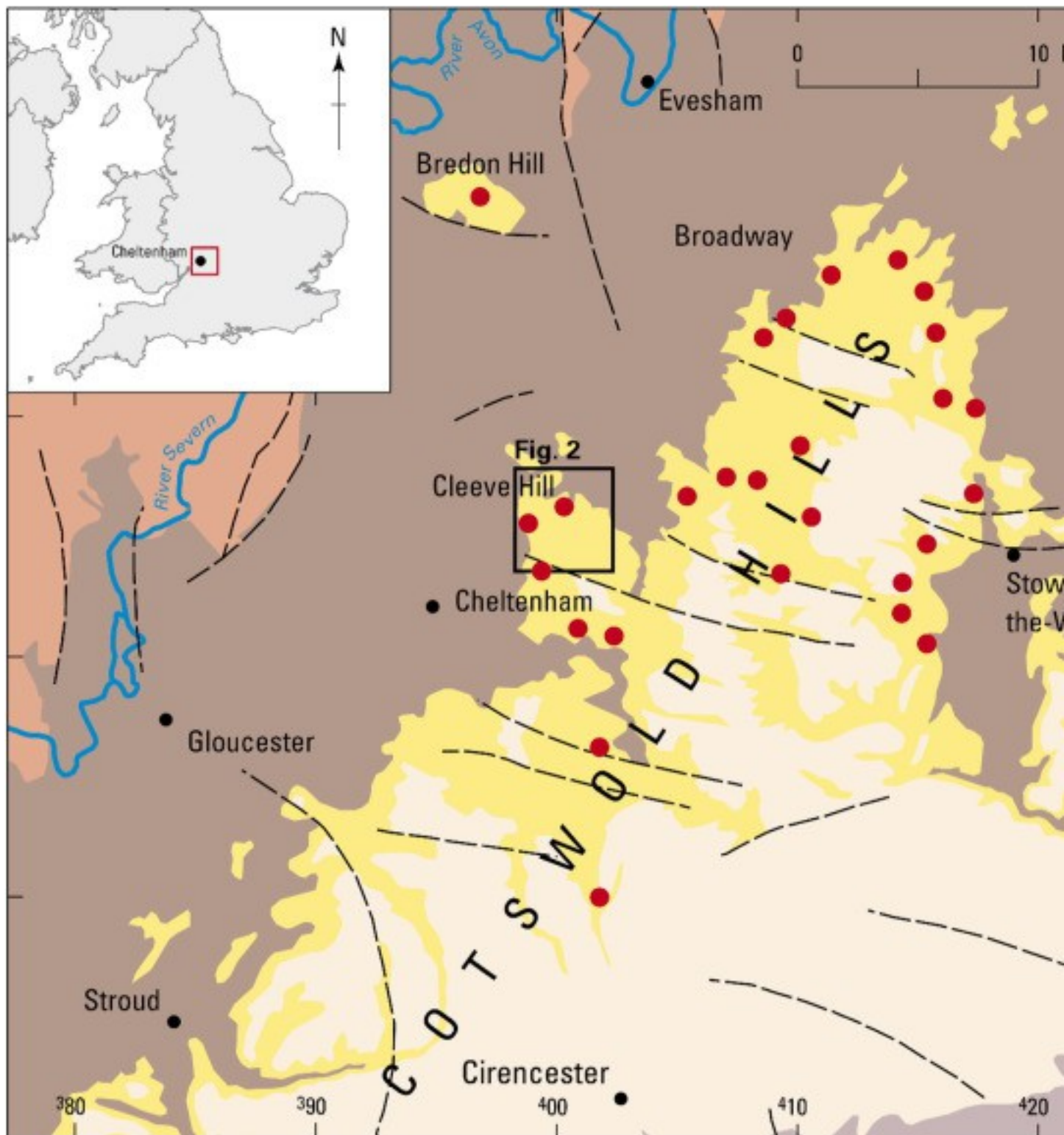
[Report a map error](#)

[Download data](#)

1. Introduction

The Cotswold Hills form a prominent north-west-facing [escarpment](#) overlooking the vale of the River Severn in the south-west English Midlands ([Fig. 1](#)), and are underlain by a succession of [limestone](#) and [mudstone](#) strata of [Jurassic](#) age. The highest point of the Hills is 330 m above OD at Cleeve Hill, near Cheltenham, close to the escarpment edge, and from here, the Hills form a highly dissected plateau generally sloping to the south-east. Between Broadway in the north and Stroud (the north Cotswolds), the crest of the escarpment is underlain along most of its length by the [Middle Jurassic](#) Inferior [Oolite](#) Group, composed predominantly of bedded ooidal limestone, overlying the Lower Jurassic Lias Group comprising mainly mudstone.

The [bedrock](#) strata generally dip gently to the south-east slightly more steeply than the plateau, and are cut by many tectonic faults with throws at surface typically of 5 to 20 m. Superficial deposits are restricted to narrow ribbons of [colluvium](#) and alluvium in valleys on the plateau, but very extensive [mass movement](#) deposits (mapped as landslides) blanket the slopes of the escarpment.



Contains Ordnance Survey data © Crown Copyright and database

— Fault
 — — — — —

■ Inferior Oolite Group
 ■ — — — — —

1. [Download high-res image \(370KB\)](#)
2. [Download full-size image](#)

Fig. 1. Regional location map. Black frame indicates area of [Fig. 2](#). Red dots indicate areas where other gull features have been mapped (BGS 1:50,000 sheets 217 and 235 only).

1.1. History of cambering research in the Cotswolds

The geology of the Cotswold Hills has been studied since the early days of [earth sciences](#), largely due to the many excellent exposures of the limestone strata in [building stone quarries](#) and their prolific included shelly fauna. From the beginning it was realised that the strata were affected by a 'derangement of strata' around Cheltenham ([Murchison, 1834](#)) and 'quaquaversals, valleyward dips and fissures' ([Hull, 1855](#)). [Richardson \(1929\)](#) also remarked on cambering features in the district including "tilting valleywards of the rock-mass (and production of open-fissure faults)" and related them to landsliding. Subsequent researches and detailed [geological mapping](#) by BGS up until the 1990's ([British Geological Survey, 1972](#), [British Geological Survey, 1998](#), [British Geological Survey, 2000](#)) revealed the widespread presence of [geomorphological features](#) that are inferred to relate to cambering and these are particularly well developed and exposed on Cleeve Hill near Cheltenham.

Cambering is very widely recognised in Great Britain, first identified in [Carboniferous](#) strata in the Pennines (references in [Ballantyne and Harris, 1994](#)), but particularly affecting [Mesozoic](#) (Jurassic to Cretaceous) strata in southern and central England ([Parks, 1991a](#), [Pook, 2013](#)), which generally comprise successions of interbedded mudstone, [sandstone](#) and limestone formations, with low regional dips (less than 5°). Cambering features and associated phenomena are caused by gradual lowering of outcropping or near-surface strata, largely under gravitational forces towards an adjacent valley. They occur where competent and permeable rocks (the 'cap-rock') overlie incompetent and impermeable beds such as mudstone or [siltstone](#). Following valley incision, the incompetent material is extruded from beneath the [cap-rock](#), in many cases in part as a result of development of a valley bulge, and initially as a result of stress relief ([Parks, 1991b](#)) but also due to a reduction in [shear strength](#) due to thawing of ice-rich rock during climatic amelioration ([Ballantyne and Harris, 1994](#)), wetting, drying, decalcification and oxidation ([Hawkins, 2013](#)). The overlying competent beds develop a local dip or 'camber' towards the valleys, and where relatively thin develop sets of many small cross-slope parallel faults separating more steeply dipping blocks (dip-and-fault structure; [Hollingworth and Taylor, 1951](#), [Hollingworth et al.,](#)

[1944](#), [Horswill and Horton, 1976](#)). In the thicker cap-rocks on the valley flanks or at the crest, sub-vertical planes of dislocation or fractures commonly develop when well-jointed, competent strata become unsupported on their downhill side following mass-movement and valley incision. Extension takes place at joints and along [bedding planes](#) with bed-over-bed sliding – including even in flat-lying or gently inclined strata. The open fractures are gulls (derived from gully), a term first used by quarrymen to describe open joints in solid strata ([Fitton, 1836](#)), a term later defined by [Hollingworth et al. \(1944\)](#) as “widened steeply inclined fissures or joints that have been wholly or partially infilled with material from above”, although infilling is not always evident or essential. ([Self, 1986](#) (for 1985)) proposed a five-fold classification for gulls, plus two hybrid styles. Although his Type E has interaction between two joints and [subsidence](#) of the intervening block, he envisages it to take place below the surface and between joints that meet at depth, not two near-vertical parallel joints forming a structure that propagates to the surface, which is the pattern we infer to occur here. This appears to merit a new movement type to add to Self's classification, but we propose that its general mechanical similarities still qualify the structure as a ‘gull’. In addition, where collapse downwards of the infill or roof results in propagation to the surface and the formation of a topographic hollow, this is termed a ‘surface gull’.

1.2. Emergence of non-invasive methods

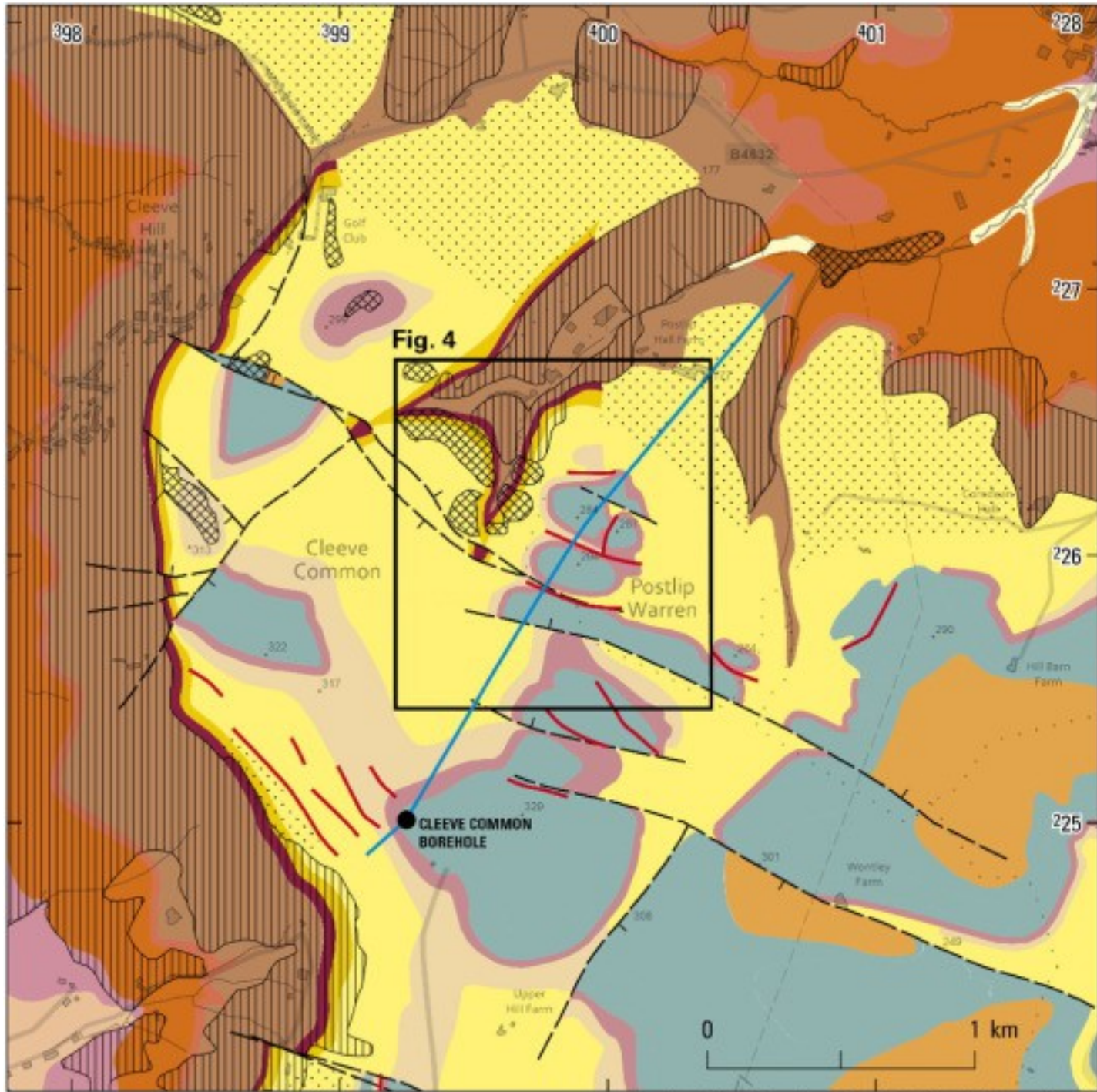
Conventional geological sampling (i.e. drilling, trenching) is usually restricted to small sampling areas (or even only single sampling points) and is comparatively expensive. Hence, its application to the investigation of complex [geological structures](#) is limited. Non-invasive geophysical techniques are able to overcome these limitations due to recent enhancements in imaging capabilities, and fast acquisition rates enabling coverage of large areas both laterally and to depth. For near-surface imaging of fractures, and sub-vertical fractures in particular, the most commonly applied geophysical techniques are electrical resistivity [tomography](#) (ERT) and ground penetrating radar (GPR) (e.g. [Carbonel et al., 2015](#), [Ercoli et al., 2012](#), [Štěpančíková et al., 2011](#), [Suski et al., 2010](#)), which are sensitive to the electrical/dielectric properties of the subsurface.

ERT is a frequently applied technique to image geomorphological processes. It is used, e.g., to characterize landslides (e.g. [Perrone et al., 2014](#)), fluvial deposition (e.g. [Chambers et al., 2014](#)) or periglacial processes (e.g. [Hauck and Kneisel, 2006](#)). Employing ERT, [Štěpančíková et al. \(2011\)](#) and [Ercoli et al. \(2012\)](#) were able to identify narrow sub-vertical fault zones from the resistivity contrast between the altered faulted

rocks and the surrounding undisturbed rock. By comparing field data with a resistivity forward model of the expected geological settings, [Suski et al. \(2010\)](#) proved the existence of an active fault zone in an urbanized area. [Carbonel et al. \(2015\)](#) defined the boundaries of a [sinkhole](#) using a joint interpretation of ERT and GPR results. Here, the displacement of the affected formations was clearly visible in the resistivity data. Although ERT can provide information on fault location, extent and dipping, it exhibits natural physical limitations, namely resolution and non-uniqueness, which can restrict the successful imaging of narrow fault zones ([Carrière et al., 2013](#)). GPR can provide better resolution of fractures and vertical features that could cause cambering (e.g. [Carbonel et al., 2014](#), [Rodríguez et al., 2014](#)) and, in comparison to ERT, provides faster [data acquisition](#) and thus smaller cost. However, its investigation depth is constrained by the resistivity of the investigated formation, where lower resistivities lead to lower penetration depths. In the case of the site at Postlip Warren, the capping formation is characterized by a comparably high clay content, showing low resistivities. Thus, the anticipated investigation depth would have been smaller than required for the study presented in this paper.

1.3. Choice of the Postlip Warren survey site

Conspicuous but enigmatic dry linear hollows, interpreted here to be surface gullies, occur at Postlip Warren ([Fig. 2](#); [Fig. 3a](#); [Fig. 4](#)), a spur on the north-east side of Cleeve Hill.



Contains Ordnance Survey data © Crown Copyright and database rights 2016

— T — Fault at rockhead, tick on downthrow side

— Mapped surface gull features

••••• Cambered areas inferred to include dip-and-fault structures

Bedrock

Salperton Limestone Formation

Aston Limestone Formation

Harford Member

1. [Download high-res image \(712KB\)](#)
2. [Download full-size image](#)

Fig. 2. Geological map of Cleeve Hill including Postlip Warren.



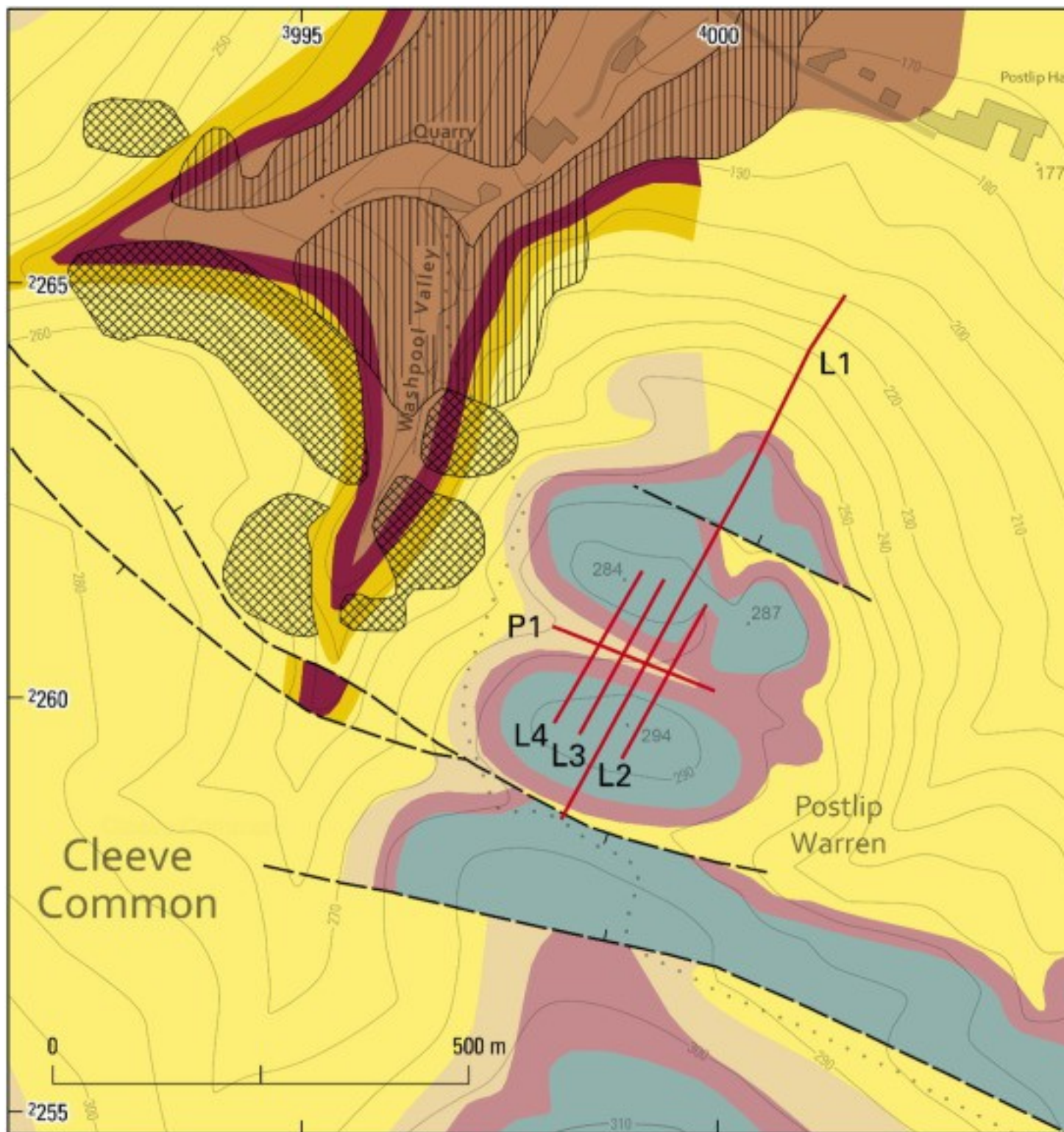
a



b

1. [Download high-res image \(278KB\)](#)
2. [Download full-size image](#)

Fig. 3. Surface gulls on Cleeve Hill: 3a Postlip Warren [SO 9984 2604]. Photographer G G Pook (P902222). 3b Cleeve Hill, view to north-west [SO 9908 2506]. Photographer A J M Barron (P902218).



Contains Ordnance Survey data © Crown Copyright and database

— T Fault at rockhead, tick on downthrow side

— Line of section

Bedrock

— Aston Limestone Formation

1. [Download high-res image \(664KB\)](#)
2. [Download full-size image](#)

Fig. 4. Geological map of Postlip Warren showing lines of resistivity traverses. Although away from the main Cotswold escarpment, and in part coincident with mapped faults thought to be of tectonic origin, the features are inferred to overlie gulls with fillings of jumbled stone, soil and some [fine-grained sediment](#), plus minor voids. A number of factors made the Postlip Warren site a prime choice for further investigation of their three-dimensional structure and testing of the ERT technique:

- The surface gulls here are some of the largest known in the district, at 500 metres long by 50 metres wide.
- The features are very distinct from the active drainage network, standing some 40 m above and open at both ends.
- The gulls form a parallel set of at least three, facilitating investigation of more than one feature.
- The affected succession is predominantly limestone and very thick for a cambered cap-rock. It is likely to be effectively dry.
- The limestone succession includes near the top a mapped bed of mudstone and is underlain by a thick mudstone formation; both should provide a contrasting resistivity signature.
- There is no significant cover of superficial deposits.
- A nearby cored [borehole](#) provides a full and detailed record of the succession affected.
- There is no significant [quarrying](#) and other intrusive human activity at the site.

The hilltop site is open grazing land largely free of obstructions and is accessible by vehicle.

1.4. Research objectives

It is widely held that cambering on escarpments is intimately related to landsliding on the adjacent slopes. However the relative and absolute timing, the causes and processes, and the resulting structures and deposits are not fully documented or understood. Current research into the age and chronology of the formation of open gulls along the Cotswold escarpment ([Farrant et al., 2015](#)) indicates that here they are over 350,000 years old, which has profound implications for any estimates of the age of the escarpment and its landslide phenomena, and the timing and processes of excavation of the Severn Valley. Gulls present potential geohazards – specifically, their disposition, form in 3D and the nature and stability of any fill have engineering implications. It is inferred that the gull fillings are sufficiently different to the intact bedrock to offer the possibility of elucidating their 3D structure and disposition using non-invasive geophysical techniques.

2. Geological reconnaissance surveys of Cleeve Hill and Postlip Warren

2.1. Geological mapping

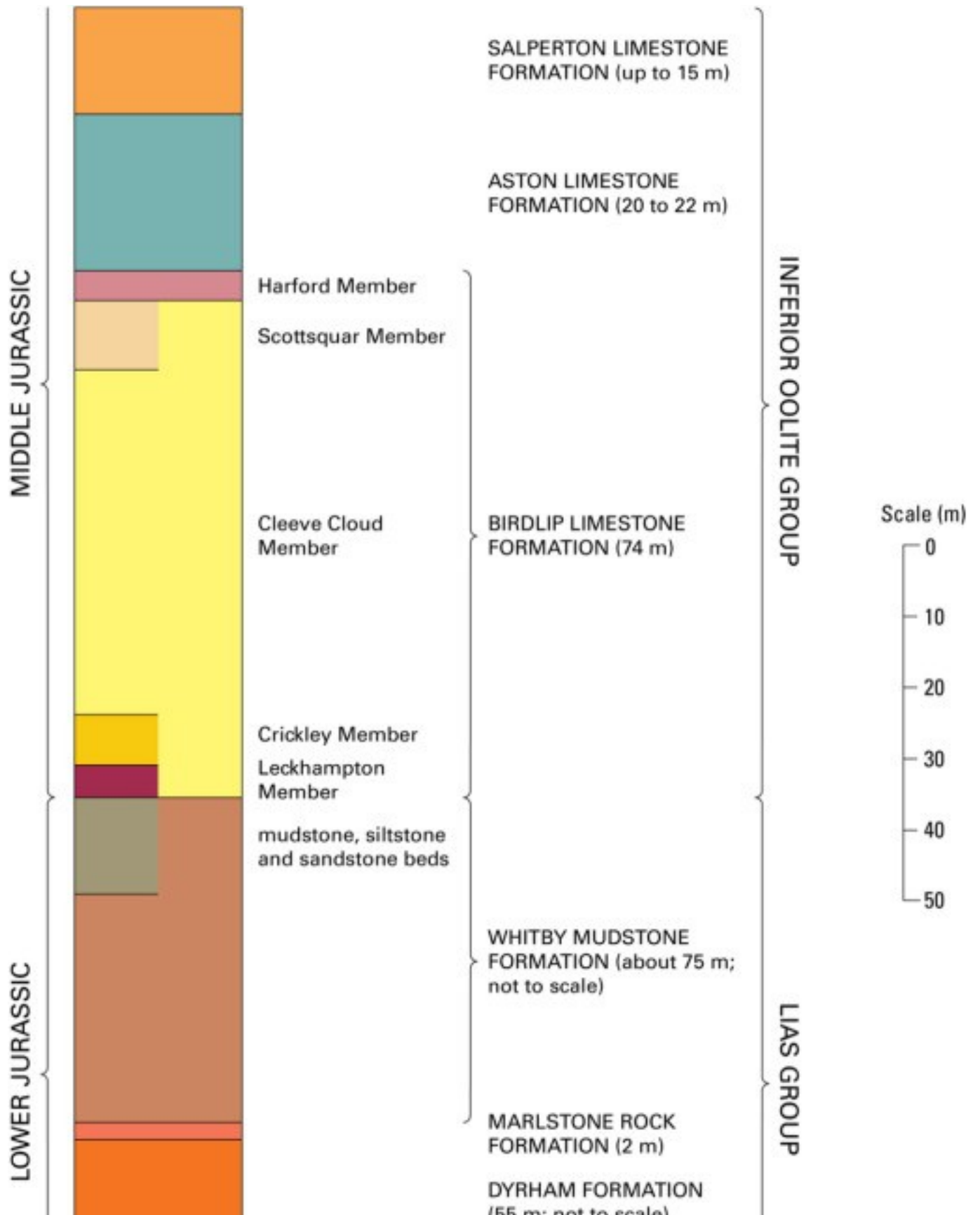
The Cleeve Hill and Postlip Warren area was geologically mapped at 1:10,000-scale by the author (AJMB) and colleague A N Morigi in 1981 and 1995. This involved field surveying on foot, recording [geomorphological features](#) and recording exposures of strata and evidence in the soil of the underlying rocks and deposits, which revealed the presence of features indicating cambering, including many surface gull structures ([Fig. 2](#); [Barron, 1999](#)), and were included in the cambering and gulls inset on the published BGS map ([British Geological Survey, 2000](#)). In preparation for the ERT survey, one of the authors (GGP) used the GeoVisionary® desktop software (<http://www.geovisionary.com/>) that enables highly flexible 3D visualisation, to undertake a [remote-sensing](#) interpretation of Postlip Warren that assisted in deciding on the ERT survey lines ([Fig. 4](#)). During further visits, observations confirmed the original 1:10,000-scale field mapping of the [bedrock](#) and the dimensions of the surface gulls.

3. Geology of Cleeve Hill and Postlip Warren

The geological context of the surface gulls and the relevant properties of the geological materials are described in the following sections.

3.1. Bedrock

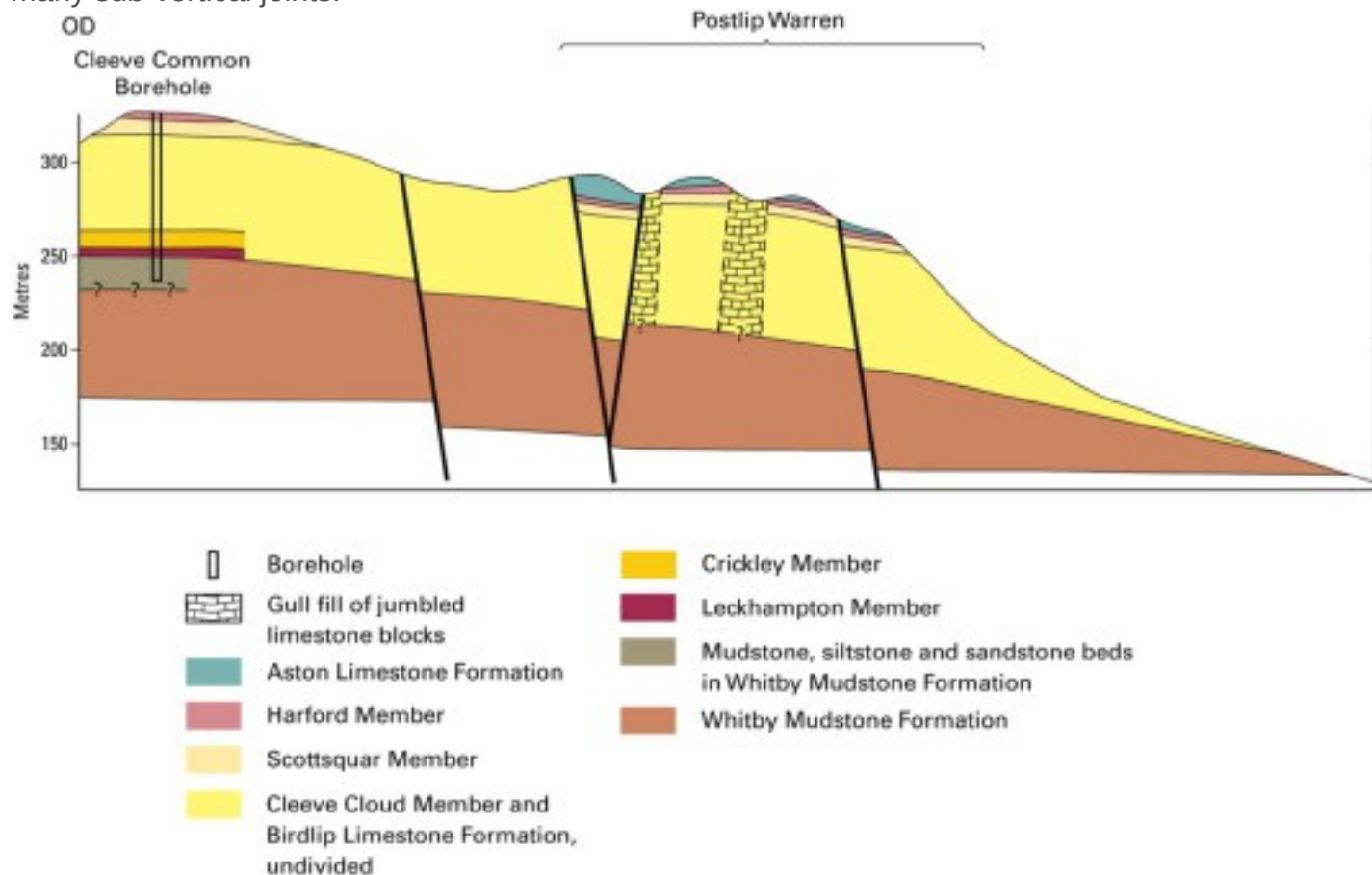
Near the [escarpment](#), the plateau of the north Cotswolds is underlain at rockhead by strata of the Inferior [Oolite](#) Group, of Middle [Jurassic](#) age ([Fig. 1](#)). The Inferior Oolite Group's three formations – in descending order the Salperton [Limestone](#), Aston Limestone and Birdlip Limestone comprise a predominantly limestone succession up to about 100 m thick at Cleeve Hill ([Fig. 5](#)). It is underlain by the Whitby [Mudstone](#) Formation of the Lower Jurassic Lias Group, here about 75 m thick.



1. [Download high-res image \(180KB\)](#)
2. [Download full-size image](#)

Fig. 5. Generalised vertical section of [bedrock](#) at Cleeve Hill and Postlip Warren. The Salperton Limestone which comprises about 15 m of limestone has limited [outcrops](#) on the Cleeve Hill plateau ([Fig. 2](#)). The Aston Limestone Formation comprises up to 22 m of shelly, sandy, ooidal limestones. Its four subdivisions widely recognisable on Cleeve Hill were not mapped on Postlip Warren where up to 20 m of strata are present.

The underlying Birdlip Limestone Formation is up to 74 m thick on Cleeve Hill. It forms the great majority of the cambered [cap-rock](#) at Postlip Warren, and comprises five distinct members that are widely mapped here ([Fig. 2](#); [Fig. 5](#)) and proved in the Cleeve Common [borehole](#) ([Fig. 6](#)). The uppermost, Harford Member is about 3 m of sand and [sandstone](#) on about 0.5 m of mudstone which is easily mappable. The four underlying members are predominantly ooidal limestone and include the 50 m-thick Cleeve Cloud Member which was a major source of [building stone](#) and is well exposed in numerous [quarries](#) on Cleeve Hill ([Fig. 7](#)). Where exposed, the formation displays many sub-vertical joints.



1. [Download high-res image \(131KB\)](#)
2. [Download full-size image](#)

Fig. 6. Cross-section of Postlip Warren including Cleeve Common [borehole](#). For line of section see [Fig. 2](#). Vertical exaggeration x4.



a



1. [Download high-res image \(717KB\)](#)
2. [Download full-size image](#)

Fig. 7. The Cleeve Cloud Member exposed at Cleeve Cloud: 7a Open joints in a face about 18 m high [SO 9842 2555]. Photographer AR Farrant (P902219). 7b. Exposed gull fill [SO 9842 2560]. Photographer A J M Barron (P902214). 7c Eroded-out gull structure on Cleeve Cloud [SO 9842 2543]. Photographer P R N Hobbs (P902216). The Whitby Mudstone Formation comprises predominantly grey silty shaly mudstone. The BGS Cleeve Common Borehole ([Fig. 6](#)) proved 13.0 m of grey silty mudstone, silt and fine-grained sandstone beds below the Inferior Oolite.

3.2. Faults

Detailed [geological mapping](#) on Cleeve Hill has enabled identification of faulting ([Fig. 2](#)) of inferred tectonic origin and of normal style, with observed dips on [fault planes](#) ranging from 50 to 70°, and displacements of up to 10 m at Postlip Warren. Some of these coincide with gull features which have evidently exploited these lines of weakness in the [bedrock](#). Importantly, mapping of the Harford Member on Postlip Warren also demonstrated the lack of vertical displacement across other surface gulls.

3.3. Superficial deposits

No superficial (Quaternary) deposits were mapped on the plateau of Cleeve Hill, although there are likely to be thin spreads of [colluvium](#) on slopes and thicker accumulations in hollows. Arguably any fills in gulls are [Quaternary](#) deposits but these are not mapped. An aim of this study is to acquire data on the properties and 3D form of any gull fill.

3.4. Joints, cambering and gull formation on Cleeve Hill

Detailed geological mapping and observation of [geomorphological features](#) indicates that the plateau of Cleeve Hill has undergone profound non-diastrorphic processes that have resulted in cambering. Undoubtedly, human activities have removed some of the evidence along the west face of the Hill. However, elsewhere, cambering phenomena include slopes where the mapped base of the Birdlip Limestone lies much further downslope than would be expected from its stratigraphical thickness, seen on the north-east side of the Hill and along the escarpment south-east of the hill-fort (stippled areas on [Fig. 2](#)). Here the limestone cap-rock thins outwards from the Hill (as in [Fig. 6](#)) and is inferred to be affected by loss of underlying mudstone thickness and the development of dip-and-fault structures, which together have resulted in significant lowering and downslope extension of the camber. However, there is no surface expression of the dip-

and-fault structures now. Notably, the slopes on the Whitby Mudstone outcrop below are commonly affected by extensive landsliding. Upslope where the cap-rock thickens (more than 20 m), in many cases surface gulls are seen crossing the slopes ([Figs. 3a, 3b](#)).

The main quarry face on Cleeve Cloud [SO 984 256] exposes a 300 m-long continuous section of at least 25 m of strata of the Birdlip Limestone Formation ([Fig. 7a](#)) cut by two or three minor faults, and displaying many open sub-vertical joints, some of which are wide enough (up to about 1.5 m) to enter – ‘gull caves’ ([Self and Boycott, 2007](#) (for 2006)). Although there are signs of dissolution on most joint faces, the gull caves are thought to have widened mechanically as they exhibit rough, broken walls with symmetrically opposing wall morphologies (‘fit features’ of [Self, 1986](#)). They tend to be vertically parallel-sided, the roof formed by trapped fallen debris or bridged by slabs in higher beds, either where there is [bedding-plane](#) slippage or the rift steps sideways, as visible in the quarry face ([Fig. 7a](#)), and the caves end where choked with boulders or rock and earth debris, or grade into impassable passages. The gull caves here show a strong [preferred orientation](#) of 120–140°, indicating lateral opening (dilation) to the south-west with, in some cases, a small component of [vertical movement](#). Other joint orientations are seen of about 070 to 080°, showing some widening, and intersections of these two sets permits divergent movement forming ‘gull tears’ ([Self, 2008](#)). These two orientations coincide closely with the vertical joint-sets J_2 and J_1 respectively, measured in the Cotswolds by [Hancock \(1969\)](#).

In addition to the caves, at one location on the quarry face of Cleeve Cloud there is a zone 10 to 15 m wide where a large, relatively coherent block of bedded limestone appears to have sunk (‘foundered’) and rotated at least 30° ([Fig. 7b](#)), although part of this inclination may be due to [cross-bedding](#). It is flanked by more disrupted masses of limestone and jumbled blocks, pockets of stony clay and earth and some minor air-filled voids. The entire mass lies between two sharp, near vertical sub-parallel joints and extends between them back into the hill. The formation and continuing development of this structure would have created a surface gull on the plateau above, which is now partially obscured. In the face, the rocks outside the zone are intact and the individual beds can be matched across indicating little vertical displacement (less than 1 m down to the south) between the walls. Comparing the main foundered mass with the walls suggests it is displaced down at least 5 m. It is inferred that this zone of displaced material extends down to the base of the Birdlip Limestone (about another 12 m), filling the space made by lateral opening, although the presence within it of large cavities cannot be discounted, and giving a cap-rock thickness here of about 25 m. The amount

of lateral opening is estimated as 2 to 4 m. This structure is regarded here as exemplifying most of the features of the gulls and surface gulls on Cleeve Hill. Nearby, a vertical notch between two intact blocks of Birdlip Limestone ([Fig. 7c](#)) is interpreted to be a gull about 2 m wide from which the fill has been eroded away. In all these instances of gulls that are too wide to be bridged, as well as the pre-existing foundered strata, other geological material would have accumulated in the resulting surface hollows. This would include limestone rubble and soil falling from the walls (colluvium) plus the gradual weathering of limestone debris and in situ development of topsoil. If recent proposals by ([Farrant et al., 2015](#)) are accepted, that gull formation along the Cotswold escarpment dates from the Middle Pleistocene and that the current summit surface of the Cotswolds is, or is close to, an exhumed pre-late Cretaceous erosion surface, this would preclude the inclusion of material derived from younger Jurassic bedrock that was removed from the Cleeve Hill area in the [early Cretaceous](#). In addition, given the topographic position on a hill top, the potential for later (Quaternary) input of further material would have been limited, apart from some hillwash and wind-blown fine sediment. Furthermore, any continued opening of the gull and/or foundering of the fill would tend to maintain the existence of the surface gull ([Fig. 3b](#)), albeit with additional infill that may differ materially from the walls.

3.5. Geophysical properties of the strata

The resistivity of rocks and soils depends on several factors, most importantly their [porosity](#), water content, and mineralogical composition, i.e. clay content ([Archie, 1942](#)). Thus significant contrasts in resistivity can be expected at site. While the capping Aston Limestone is highly weathered, the limestones of the Birdlip Limestone Formation form a competent unit with low porosity ([Besien et al., 2006](#)) and are likely to exceed resistivities of more than 1 k Ω m ([Telford et al., 1990](#)). Due to the higher porosity and clay content the resistivity of the Aston Limestone will be lower. As the Harford Member is characterized by poorly compacted sandstone and a thin layer of mudstone (0.5 m) its resistivity is likely to be an order of magnitude lower (i.e. $\sim 100 \Omega$ m) than the competent limestone formations. The Whitby Mudstone Formation has large clay content, which in turn forms the lowest resistivities at site ($\sim 10 \Omega$ m). As gulls are characterized by rotated, fractured and collapsed limestone blocks forming large voids, these structures will have a different resistivity than the surrounding rock formations.

4. Geomorphology of Postlip Warren

Postlip Warren forms a broad spur up to 294 m aOD (above Ordnance Datum) on the east side of the Cleeve Hill plateau, flanked on the west and east sides by deep V-shaped valleys cut down to the Whitby [Mudstone](#) by the [headwaters](#) of the River Isbourne. These streams are fed by springs issuing from the base of the Birdlip [Limestone](#). The steeper, west side of the Warren slopes into the Washpool Valley about 90 m below, the eastern flank grades more gently down by over 100 m. Landslides affect the lower slopes of both valleys, and the Birdlip Limestone has been quarried leaving extensive waste heaps in the Washpool Valley ([Fig. 4](#)). The crest of the Postlip Warren spur is cut right across by two sub-parallel linear hollows, plus two further, shorter hollows; one near parallel and one at right angles joining two of the longer ones, which are well-defined by the mapped [outcrops](#) of the Harford Member (see [Section 3.1](#) above). All are U-shaped and dry and are inferred to overlie gull structures. The two major hollows are up to 500 m long, 50 m wide and the floors are up to 10 m below the intervening ridges ([Fig. 3a](#)). They are open at both ends, hanging above the valleys, although there are depressions in the valley sides running from the ends of the hollows down to the valley floors, possibly indicating more easily erodible substrates. The Warren is rough pasture, but the grass in the floors of the hollows is lusher, implying deeper, more moisture-retentive soil. Notably, to the south and up-slope on Cleeve Common, there are three further parallel surface gulls ([Fig. 2](#)).

5. Geophysical reconnaissance surveys

As significant contrasts in resistivity were expected between the competent and cambered strata, electrical resistivity [tomography](#) (ERT) was used to compare subsurface characteristics with surface features and to image the geological formations forming the gulls at site.

2D ERT measurements are usually conducted by introducing an electrical field into the ground through point-like [electrodes](#) at one location and measuring a corresponding [voltage](#) at a different location. By making measurements at different locations, and with different spacings between injection and voltage dipole, a 2D resistivity section can be created. The measured data are an apparent resistivity, which represents an averaged value of the true resistivity distribution. To obtain a true resistivity model, these measured apparent resistivities form the basis for an inverse modelling procedure. Starting from a homogeneous resistivity model (i.e. with the mean of measured data) this model is iteratively altered until its response explains the measured data reasonably well ([Loke et al., 2013](#)).

It should be noted that ERT models are smoothed images of a true resistivity distribution and that model resolution decreases with increasing depth of investigation (caused by a smaller amount of data constraining the model). Off-line resistivity or topographic features may violate the underlying 2D assumption (i.e. survey orientation perpendicular to the strike of the structure) and thus interpretation of 2D ERT models may be complicated if such features exist ([Loke et al., 2013](#)). Therefore, ERT models can only provide an approximation of the true resistivity and subsurface geometries ([Olayinka and Yaramanci, 2000](#)), highlighting the need for calibration and interpretation using other sources of ground truth and comparison to [forward modelling](#) results.

The ERT survey was undertaken during July 2013. ERT data were collected using an AGI SuperSting R8 IP system attached to up to 84 stainless steel electrodes via multicore cables. This multi-channel resistivity metre allows [voltage measurement](#) at 8 different positions simultaneously. Ground conditions were generally very dry and the [soils cover](#) above the Aston [Limestone](#) very thin. To improve the electrical contact to the ground and thus also the data quality, each electrode was watered using a saline solution. Electrode positions were surveyed using real-time [kinematic](#) (RTK) [GPS](#) with centimetric accuracy. This data were then used to estimate grid location and elevation of each electrode which was incorporated into the inversion.

For the geophysical investigation of the Postlip Warren five lines have been employed; their locations are shown in [Fig. 4](#). Four of these lines (L1–L4) have been orientated perpendicular to the gulls, while P1 was located along the axis of one. Line L1 is the longest line stretching over 722 m with an electrode spacing of 5 m and thus crossing two suspected gulls. Although a third and prominent surface gull was traversed at its southern-most end, only minor information could be obtained from it. This is due to the limited resolution towards the end of the line, a characteristic feature of resistivity imaging. With an investigation depth of about 80 m we were able to image the three formations occurring at site. L2 to L4, and P1 were 205 m long, had an electrode spacing of 2.5 m and were located to cross the most prominent gull at the Postlip Warren, providing a higher model resolution at this area compared to L1. These lines had an investigation depth of 35 m. A dipole-dipole measurement configuration was employed for each of the lines. L1 was surveyed using (along-surface) dipole lengths (a) of 5, 10, 15, 20, 25, 30 and 35 m and dipole separations (na) of $1a$ to $8a$. To allow measurements on 149 electrodes, a roll-along procedure was used employing 84 electrodes at each step. For profiles L2 to L4, and P1 dipole lengths of 2.5, 5, 7.5, 10, 12.5 and 15 m and dipole separations of $1a$ to $8a$ were used.

For quality assessment, the dipole-dipole command sequence comprised both normal and reciprocal (i.e. interchange of injection and voltage dipole) measurements. Theoretically, these measurements should return the same resistivity. By comparing the value of the two measurements a reciprocal error can be determined, which is proven to be a robust and reliable means of assessing ERT data quality. During the course of the survey 36,908 measurements were made, corresponding to 18,454 reciprocal pairs.

A summary of the [contact resistances](#) and reciprocal error characteristics of the ERT lines are shown in [Table 1](#). The very dry [soil conditions](#) and thin soil cover are reflected by relatively high contact resistances, with mean values ranging from about 900 Ω to 7000 Ω . Nevertheless, the reciprocal errors show reasonable data quality with more than 50% of the data having errors smaller than 1% and more than 85% of the data with errors less than 5%. Data points with a reciprocal error of more than 5% were removed from the data set and the errors were used to weight the data during the inversion. The resulting ERT models show a good agreement between model response and measured data, with root-mean-squared (RMS) errors lower than 2.6%. Note that the largest misfit remains for L4, at which the highest contact resistances and reciprocal error levels were recorded.

Table 1. [Contact resistance](#) and reciprocal error summary information for ERT Lines.

	Number of measurements ^a	Contact resistance (Ohms)		Fraction (%) of data set below reciprocal error level		RMS model-data misfit (%)
		Mean	SD ^b	1%	5%	
L1	6694	3449.47	3373.78	70.39	92.87	2.34
L2	2940	2988.73	2623.54	81.09	95.71	1.00
L3	2940	6061.00	6383.78	62.28	89.97	1.07
L4	2940	7161.58	5122.55	49.59	85.48	2.58
P1	2940	919.30	220.28	89.73	90.51	1.03

a

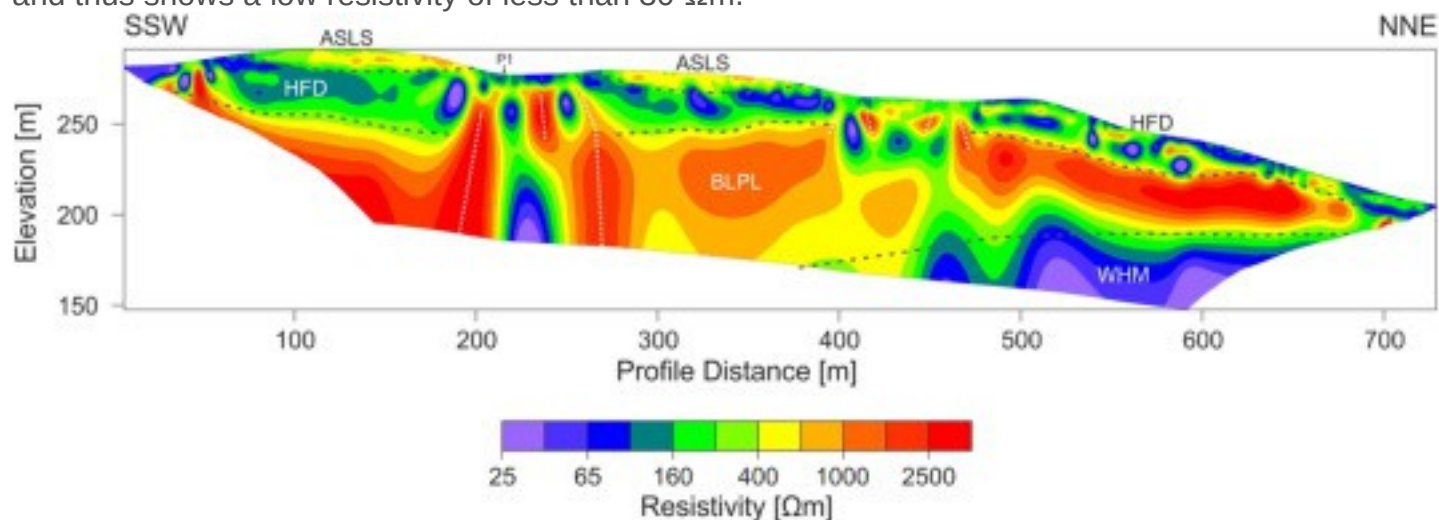
Each comprising reciprocal pair (i.e. forward and reciprocal measurement).

b

Standard deviation (SD).

6. Results of ERT survey

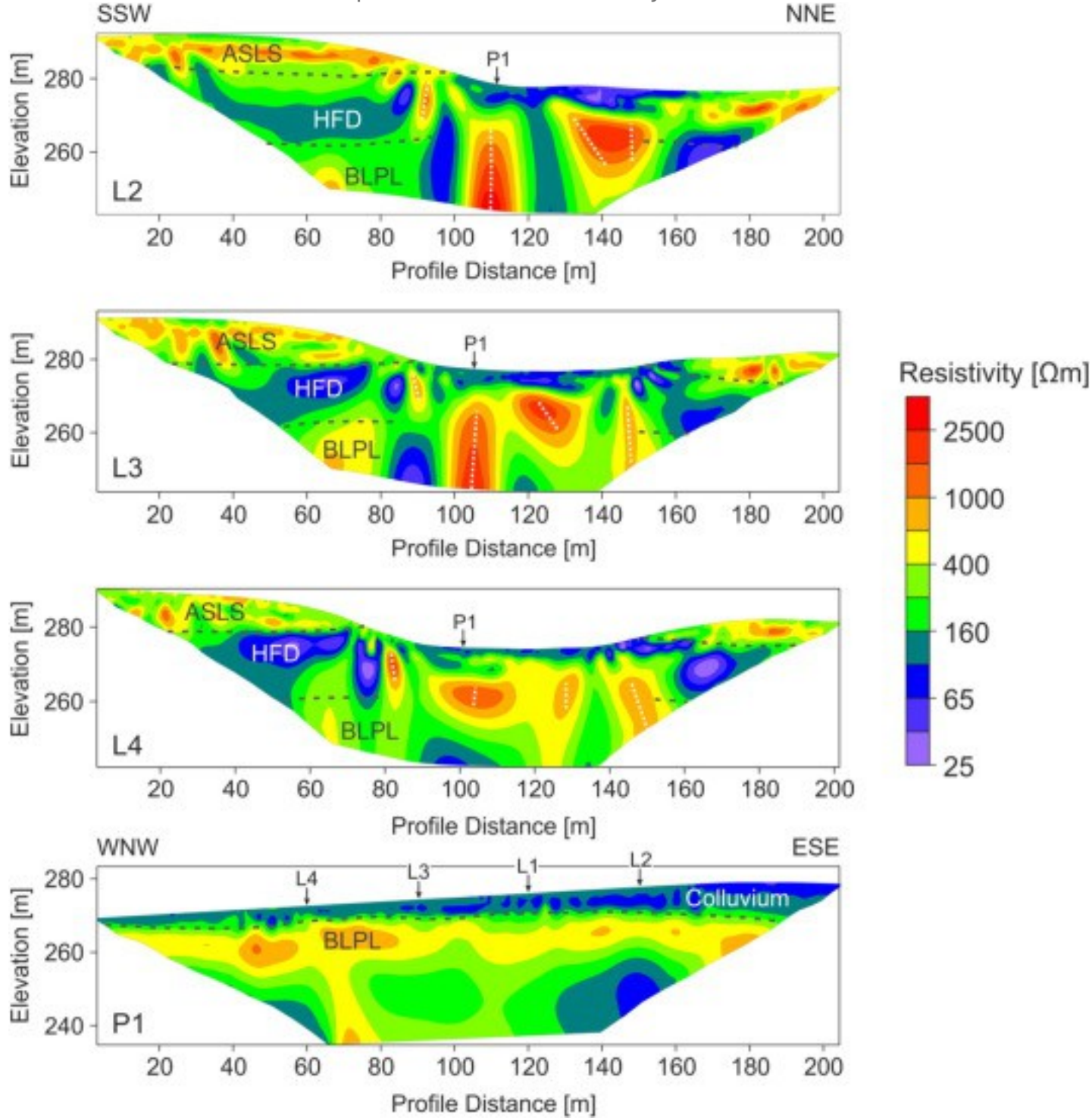
The [geophysical survey](#) of L1 ([Fig. 8](#)) provides information about the deeper geology at the site, imaging the main formations and units. The resistivity models of L2 to L4, and P1 can be used to follow the structural features characterising the gull ([Fig. 9](#)). In these profiles cold colours indicate low resistivities ($< 100 \Omega\text{m}$), corresponding to material with higher clay content and less [consolidation](#), such as [colluvium](#) and the sand and [mudstone](#) beds of the Harford Member. Warm colours, such as yellow and red, show the high resistivities ($> 500 \Omega\text{m}$) of the competent and weathered [limestone](#). The lithological boundaries indicated in [Fig. 8](#) relate very well with the mapped [bedrock](#) geology as shown in [Fig. 4](#), and are thus in agreement with the local stratigraphy. The deeper limestone members of the Birdlip Limestone Formation show a rather homogeneous structure with resistivities ranging between 1000 and 3500 Ωm . The capping Aston Limestone, however, shows a much more heterogeneous structure with smaller resistivity values (between 200 and 1000 Ωm), thus highlighting the weathering of this formation. This heterogeneity has also been imaged in the adjacent profiles L2 to L4 in [Fig. 9](#). Due to the higher resolution of these profiles, the non-uniform structure of the Aston Limestone is even more pronounced. The lithological difference of the Harford Member and its overlying and underlying limestones provides a clear resistivity contrast in the geophysical profiles, with resistivities well below 300 Ωm . The boundary between the Aston Limestone and Harford Member becomes less apparent with a profile distance of more than 475 m along L1, where high and low resistive features alternate, and a minor fault crosses the section. Towards the northern end of L1 it was also possible to image the upper boundary of the Whitby Mudstone Formation underlying the Birdlip Limestone. This mudstone is characterized by high clay content and thus shows a low resistivity of less than 30 Ωm .



1. [Download high-res image \(133KB\)](#)

2. [Download full-size image](#)

Fig. 8. Interpreted ERT section of profile L1. Dark dashed lines indicate stratigraphical boundaries, white dashed lines indicate discontinuities. ASLS – Aston [Limestone](#), HFD – Harford Member, BLPL – Birdlip Limestone, WHM – Whitby [Mudstone](#).

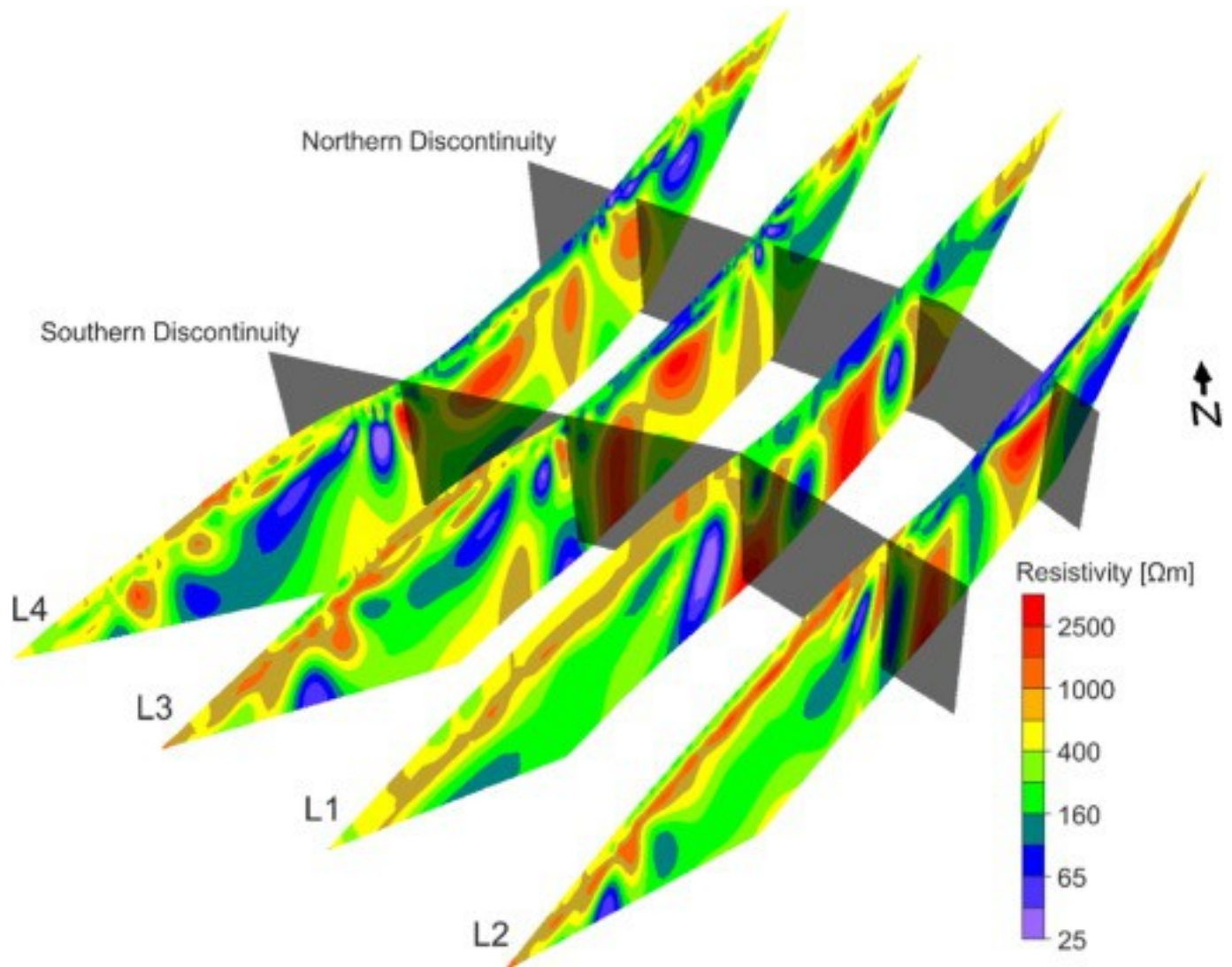


1. [Download high-res image \(345KB\)](#)

2. [Download full-size image](#)

Fig. 9. Interpreted ERT sections of profiles L2, L3, L4, and P1. Dark dashed lines indicate lithological boundaries, white dashed lines fractures. ASLS – Aston [Limestone](#), HFD – Harford Member, BLPL – Birdlip Limestone.

We have interpreted sub-vertically aligned structures by tracing lines through the zones of highest resistivity in Lines L1 to L4 ([Fig. 8](#), [Fig. 9](#)), most of which are inferred to correspond with vertical discontinuities (see [Section 7](#)). These structures are more dominant and deeper-seated in the southern gull (at a profile distance of about 225 m along L1), which also has the largest surface expression, and interestingly the fractures on the southern (200 m) and northern (260 m) sides appear to dip steeply to the south and north respectively. Using profiles L2 to L4, the geometry of these features can be followed through the gull. Bounding discontinuities have been highlighted by black planes in the fence diagram shown in [Fig. 10](#). The discontinuity that bounds the gull in the south is located at about 85 to 90 m, and changes its dip from southerly in L2 to northerly in L4. Its resistivity signature shown in L1 (190–200 m) indicates that it is a deep-seated structure. The most prominent and deepest feature is located at about 110 m along L2, at the topographically lowest point in the gull. From L2 to L3 (which are separated by 60 m) its signature hardly changes, but it becomes less prominent in L4, which may correspond to a change in the nature of the gull fill at depth – possibly its water content. Together with the intermediate features at 230 m in L1 and 130 m in L3 and L4 these are inferred to be a median zone of chaotic material, rather than bounding planes.



1. [Download high-res image \(252KB\)](#)
2. [Download full-size image](#)

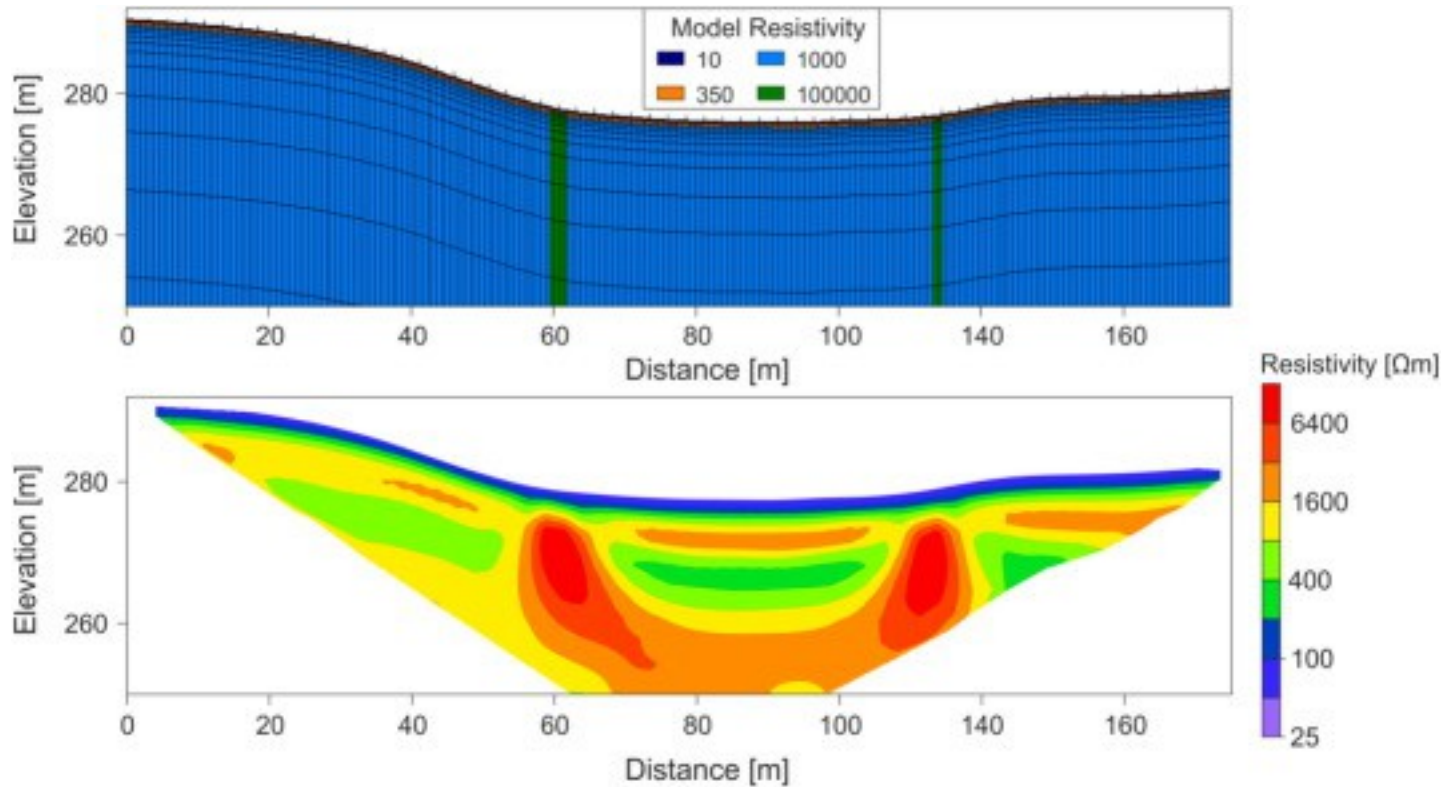
Fig. 10. 3D fence diagram of the four north-south ERT profiles. Black planes indicate the southern and northern discontinuities which form the boundary of the gull structure. NB: only part of section L1 is shown.

The high resistive anomaly in L2 at 135–150 m may be related to discontinuities beneath the cross-cutting downslope hollow – subsurface structures at this intersection are likely to be complex or even chaotic. Conspicuous features at 150 m in L3 and L4 appear to be northward-dipping, and comparison with L1 suggests that these fractures may be connected to a deep-seated structure. These features are likely to form the northern boundary of the gull (see [Fig. 10](#)).

Profile P1, as elongated along the strike of the fractures, does not show any evidence of these structures. However, it indicates a thinning of the colluvium towards the western end of the section and shows the underlying collapsed and disrupted Birdlip Limestone.

7. Discussion

Due to the limitations of the inversion process of ERT, i.e. smoothing of the resistivity models, fractures are not easily imaged nor interpreted. For resistivity measurements an open fracture is equivalent to an isolator, thus current will not pass this region and the data will contain only minimal information about its presence. To understand the effects such fractures will cause in the ERT models, numerical [forward modelling](#) was employed to create synthetic data which were then inverted using the same constraints as for the field data. The resistivity forward model and the inverted resistivity model arising from the synthetic data are shown in [Fig. 11](#). The model resembles a simplified geological section, with a very thin layer of overburden ($\rho = 10 \Omega\text{m}$, 0.5 m thick) covering weathered [limestone](#) ($\rho = 350 \Omega\text{m}$, 1.5 m thick), which is overlying competent limestone [bedrock](#) ($\rho = 1 \text{ k}\Omega\text{m}$). In the model the local topography of L3 has been employed. The trough in the middle of the model indicates the gull, which is bounded by two vertical features. These are assumed to be mostly air-filled fractures and therefore a large resistivity of $\rho = 100 \text{ k}\Omega\text{m}$ has been assigned to them. Although not shown in [Fig. 11](#), the model extends down to about 70 m. The [electrode](#) arrangement used to create the synthetic data is similar to the field arrangement used at L3, i.e., electrode spacing of 2.5 m, dipole lengths (a) of 2.5, 5, 7.5, 10, and 12.5 m, and dipole separations (n) of 1 to 8. The amount of employed electrodes was 64 – slightly smaller than in the field acquisition.



1. [Download high-res image \(195KB\)](#)
2. [Download full-size image](#)

Fig. 11. Resistivity forward model (top) used to create a synthetic data set. Green structures represent deep-seated discontinuities. (bottom) Resistivity model obtained by inverting synthetic data. High resistive structures at a distance of 60 m and 125 m correspond to the modelled discontinuities.

The inverted resistivity model arising from the synthetic data shows very similar features to what is imaged in [Fig. 8](#), [Fig. 9](#). The two vertical features cause a heavily distorted resistivity model, with areas of under- and overestimation of the true resistivity. Both, however, are successfully imaged as near vertical, although not as sharply as, and with less resistivity contrast than in, the forward model. Also, these features extend not as deep as in the model. To both sides of the features, areas of low resistivity arise, which are also caused by the disturbance of the current flow by the vertical insulators. These low resistive features can also be seen in lines L1 to L4, decreasing the low resistivity of the Harford Member. Additionally, the resistivity model in [Fig. 10](#) shows a low resistive area between the two fractures, which is similar to features that can be found in the field data (e.g. L1 at a profile distance of 215 m).

Informed by this modelling study, the features imaged on Postlip Warren can be interpreted as highly resistive, near-vertical fractures with a significant amount of air-

filled voids, forming opposing parallel pairs. The filling between these structures is most likely to be formed of blocks and rubble of limestone and less likely to consist of soil, fine-grained material and highly weathered limestone. Although the field data show them as high resistive areas with a broad extent (up to 50 m wide), these ERT model values can be caused by cambering structures only 1 to 5 m wide. Note that, although, the studied structures are likely to show 2.5D characteristics (i.e. small variation in strike direction), 3D topographical and subsurface features may have led to artefacts in the ERT data.

From this interpretation, and by comparison with observations of nearby exposed phenomena ([Fig. 7b](#)), we infer that the surface gulls on Postlip Warren are underlain by graben-like structures with vertical or possibly overhanging walls, and extend at least to the base of the Birdlip Limestone succession, at a depth of about 80 m. They occupy almost the full width of the bottom of the hollows they underlie, and are filled with a semi-chaotic jumble of Birdlip Limestone material including some air-filled voids. Although their geometry indicates that their bounding surfaces may not coincide in 3D with normal tectonic faults along a similar alignment, any pre-existing fault plane or zone is likely to have been exploited and incorporated in the fill of disrupted bedrock material.

7.1. Development of gull structure

The sets of vertical joints present in the Middle Jurassic limestone strata of the Cotswolds ([Hancock, 1969](#)) are regarded as resulting from the release of residual [strain](#) energy attendant on uplift. Major phases of uplift in this region occurred in the [latest Jurassic](#) to [early Cretaceous](#) ([Chadwick, 1986](#)), and [Palaeogene](#) ([King, 2006](#)), and thus the pervasive networks of joints in the Inferior [Oolite](#) strata are inferred to predate the development of the Cotswold [escarpment](#) in the Middle Pleistocene ([Farrant et al., 2015](#)). Following this, the sequence of events that resulted in formation of the gull structures here is thought to be as follows:

1.

Formation of the spur of Postlip Warren through deep incision of the local drainage network under high precipitation, runoff and spring discharge, leading to spring sapping and mass wastage under cycles of Pleistocene periglacial and interglacial conditions, forming V-shaped ravines up to 100 m deep with slopes of up to about 20°. Tectonic faults and joints already present in rock mass.

2.

Excavation of valleys leads to reduction of lateral support of the mass of Birdlip Limestone strata forming the spur.

3.

Reduction in [shear strength](#) in the underlying Whitby Mudstone (see [Introduction](#)) leads to it behaving in a plastic manner and volume is lost by [extrusion](#), particularly close below the boundary with the permeable and saturated [cap-rock](#).

4.

This further loss of support below permits extension of the Birdlip Limestone mass by creep under gravity towards the surrounding valleys by lateral opening of sub-vertical joints that penetrate to its full depth. Although mainly towards the NNE the presence within the spur of at least one gull at right angles (downslope) implies a component of spreading into the side valleys has occurred.

5.

Opening occurs along parallel sets (pairs or multiples) of fractures that are closely-spaced (up to about 30 m). Dilation by a moderate (2 to 5 m) amount in total within these sets may be enough to destabilise the infilling stack of rock, which topples and/or collapses sideways into the new space. The resulting chaotic material, including many voids, has a much increased resistivity, which is clearly imaged by the ERT survey. Where the gull meets the valley side, material may fall outwards.

6.

Collapse of the fill produces a hollow at the surface. This may be sudden or incremental.

7.

Over time, any dog-legs in gulls are likely to be smoothed and masked by breakdown of the shoulders of the hollows, providing gull fill material. Further degradation of the fill, accumulation of wind-blown material and soil formation generates a continuous cover, which is smoothed by later processes including trampling by grazing animals and human earthwork construction and land management activities, likely also to degrade the shoulders of the hollows.

8. Conclusions and further research

The combination of detailed [geological mapping](#), observation and interpretation of [geomorphological features](#) and analysis of ERT data has elucidated much of the nature of these landscape phenomena. It is reasonable to infer that similar surface gulls elsewhere on Cleeve Hill and in the wider north Cotswolds are underlain by similar structures, e.g. at Broadway Tower [SP 114 363] ([Barron et al., 2002](#), pl. 5), and similar ERT investigations of these would further test and help refine the methodology. In addition, for comparison, other non-invasive geophysical techniques (such as micro-seismicity and ground penetrating radar) should be tried out on Postlip Warren to evaluate their merits. Other known occurrences of gulls in the south Cotswolds have little or no surface expression, either because they have a cemented capping, or because they do not penetrate to the surface above ([Farrant et al., 2015](#), [Hawkins, 2013](#), [Self, 2008](#)). The latter are mostly known from caving explorations or mine-workings that intercept them, so can be accurately located at depth in cave or mine surveys, and sometimes form intricate grid sets. These should be investigated using surface ERT surveys to evaluate the technique to locate otherwise hidden features. Additionally, the imaging of the features at Postlip can be compared with results obtained at other sites which lack the surface features but where cambering is suspected.

Acknowledgements

The co-operation of the landowners, Richard, Dawn and Edward Albutt, and the Cleeve Common Board of Conservators warden David Stevenson is gratefully acknowledged. The authors benefitted from useful discussions in the field and the office with Peter Hobbs, Andrew Farrant and John Chambers (all BGS) and thanks are due to Milene Astoul and Maxence Perraud for assistance during the survey. [Fig. 1](#), [Fig. 2](#), [Fig. 4](#), [Fig. 5](#), [Fig. 6](#) drawn by Ian Longhurst (BGS).

A J Mark Barron, Seb Uhlemann and Lucy Oxby publish with the permission of the Executive Director, British [Geological Survey](#) (Natural Environment Research Council), and Geoff Pook with the permission of Cardiff University.

Appendix A. Supplementary data

The following KMZ file contains the Google map of the most important areas described in this article.

[Download Keyhole Markup file \(1000KB\)Help with kmz files](#)

Map. KMZ file containing the Google map of the most important areas described in this article.

References

[Archie, 1942](#)

G.E. Archie **The electrical resistivity log as an aid in determining some reservoir characteristics**

Pet. Trans. AIME, 146 (1942), pp. 54-62

[CrossRefView Record in Scopus](#)

[Ballantyne and Harris, 1994](#)

C.K. Ballantyne, C. Harris **The Periglaciation of Great Britain**

Cambridge University Press, Cambridge (1994)

[Barron, 1999](#)

A.J.M. Barron **Geology of the Bishop's Cleeve area (SO 92 NE)**

British Geological Survey Technical Report, WA/99/01 (1999)

[Barron et al., 2002](#)

A.J.M. Barron, M.G. Sumbler, A.N. Morigi **Geology of the Moreton-in-Marsh district - a brief explanation of the geological map**

Sheet Explanation of the British Geological Survey (2002)

ISBN Sheet 217 (England and Wales)

[Besien et al., 2006](#)

A. Besien, A. Pearson, M. Boland, S. Cone **Groundwater quality review: cotswold edge jurassic limestone**

Environment Agency (2006)

GWQR-MID-G9 (Bristol)

[British Geological Survey, 1972](#)

British Geological Survey **Gloucester. England and Wales Sheet 234. Solid and Drift. 1:50000 Geology Series**

British Geological Survey, Keyworth, Nottingham (1972)

[British Geological Survey, 1998](#)

British Geological Survey **Cirencester. England and Wales Sheet 235. Solid and Drift. 1:50000 Geology Series**

British Geological Survey, Keyworth, Nottingham (1998)

[British Geological Survey, 2000](#)

British Geological Survey **Moreton-in-Marsh. England and Wales Sheet 217. Solid and Drift. 1:50000 Geology Series**

British Geological Survey, Keyworth, Nottingham (2000)

[Carbonel et al., 2014](#)

D. Carbonel, V. Rodriguez, F. Gutierrez, J.P. McCalpin, R. Linares, C. Roque, M. Zarroca, J. Guerrero, I. Sasowsky **Evaluation of trenching, ground penetrating radar (GPR) and electrical resistivity tomography (ERT) for sinkhole characterization**

Earth Surf. Process. Landf., 39 (2014), pp. 214-227

[CrossRefView Record in Scopus](#)

[Carbonel et al., 2015](#)

D. Carbonel, V. Rodriguez-Tribaldos, F. Gutierrez, J.P.Galve, J. Guerrero, M. Zarroca, C. Roque, R. Linares, J.P. McCalpin, E. Acosta **Investigating a damaging buried sinkhole cluster in an urban area (Zaragoza city, NE Spain) integrating multiple techniques: geomorphological surveys, DInSAR, DEMs, GPR, ERT, and trenching**

Geomorphology, 229 (2015), pp. 3-16

[ArticleDownload PDFView Record in Scopus](#)

[Carrière et al., 2013](#)

S.D. Carriere, K. Chalikakis, G. Senechal, C. Danquigny, C. Emblanch **Combining electrical resistivity tomography and ground penetrating radar to study geological structuring of karst unsaturated zone**

J. Appl. Geophys., 94 (2013), pp. 31-41

[ArticleDownload PDFView Record in Scopus](#)

[Chadwick, 1986](#)

R.A. Chadwick **Extension tectonics in the Wessex Basin, southern England**

J. Geol. Soc. Lond., 143 (1986), pp. 465-488

[CrossRefView Record in Scopus](#)

[Chamb](#)

[ers et](#)

[al.,](#)

[2014](#)

J.E. Chambers, P.B. Wilkinson, S. Uhlemann, J.P.R.Sorensen, C. Roberts, A.J. Newell, W.O.C. Ward, A. Binley, P.J.Williams, D.C. Goody, G. Old, L. Bai **Derivation of lowland riparian wetland deposit architecture using geophysical image analysis and interface detection**

Water Resour. Res., 50 (2014), pp. 5886-5905

[CrossRefView Record in Scopus](#)

[E
r
c
o
l
i
e
t
-
a
l
.](#)

-
2
0
1
2

M. Ercoli, C. Pauselli, E. Forte, L. Di Matteo, M. Mazzocca, A. Frigeri, C. Federico **A multidisciplinary geological and geophysical approach to define structural and hydrogeological implications of the Molinaccio spring (Spello, Italy)**

J. Appl. Geophys., 77 (2012), pp. 72-82

[ArticleDownload PDFView Record in Scopus](#)

[Farrant
et al.,
2015](#)

A.R. Farrant, S.R. Noble, A.J.M. Barron, C.A. Self, S.Grebbby **Speleothem U-series constraints on scarp retreat rates and landscape evolution: an example from the Severn valley and Cotswold Hills gull-caves, UK**

J. Geol. Soc. Lond., 172 (2015), pp. 63-76

[CrossRefView Record in Scopus](#)

[Fitton, 1836](#)

W.H. Fitton **Observations on some of the strata between the Chalk and the Oxford Oolite in the South-East of England**

Trans. Geol. Soc., 2 (1836)

[Hancock, 1969](#)

P.L. Hancock **Jointing in the Jurassic limestones of the Cotswold Hills**

Proc. Geol. Assoc., 80 (1969), pp. 219-241

[ArticleDownload PDFView Record in Scopus](#)

[Hauck and Kneis](#)

C. Hauck, C. Kneisel **Application of capacitively-coupled and DC electrical resistivity imaging for mountain permafrost studies**

Permafr. Periglac. Process., 17 (2006), pp. 169-177

[CrossRefView Record in Scopus](#)

[Hawkins, 2013](#)

A.B. Hawkins **Engineering significance of superficial structures and landslides in the Bath area, UK**

Bull. Eng. Geol. Environ., 72 (2013), pp. 353-370

[CrossRefView Record in Scopus](#)

[Hollingworth and](#)

S.E. Hollingworth, J.H. Taylor **The Northamptonshire Sand Ironstone: Stratigraphy, Structure and Reserves**

Memoirs of the Geological Survey of Great Britain, The Mesozoic Ironstones of England (1951)

[Hollingworth et al](#)

S.E. Hollingworth, J.H. Taylor, G.A. Kellaway **Large-scale superficial structures in the Northamptonshire ironstone field**

Q. J. Geol. Soc. Lond., 100 (1944), pp. 1-44

[CrossRefView Record in Scopus](#)

[Horswill and Hor](#)

P. Horswill, A. Horton **Cambering and valley bulging in the Gwash valley at Empingham, Rutland**

Philos. Trans. R. Soc. Lond., A283 (1976), pp. 427-462

[CrossRefView Record in Scopus](#)

[Hull, 1855](#)

E. Hull **On the physical geography and Pleistocene phenomena of the Cotteswold Hills**

Q. J. Geol. Soc. Lond., 11 (1855), pp. 475-496

[King, 2006](#)

C. King **Paleogene and neogene: uplift and a cooling climate**

P.J. Brenchley, P.F. Rawson (Eds.), The geology of England and Wales, Geological Society, London (2006)

[Loke et al., 2013](#)

M.H. Loke, J.E. Chambers, D.F. Rucker, O. Kuras, P.B. Wilkinson **Recent developments in the direct-current geoelectrical imaging method**

J. Appl. Geophys., 95 (2013), pp. 135-156

[ArticleDownload PDFView Record in Scopus](#)

[Murchison, 1834](#)

R.I. Murchison **Outline of the Geology of the Neighbourhood of Cheltenham**

Davies, Cheltenham (1834)

[Olayinka and Ya](#)

A. Olayinka, U. Yaramanci **Assessment of the reliability of 2D inversion of apparent resistivity data**

Geophys. Prospect., 48 (2000), pp. 293-316

[CrossRefView Record in Scopus](#)

[Parks, 1991a](#)

C.D. Parks **Cambering and Valley Bulging in England**

University of Newcastle, Ph D thesis (1991)

[Parks, 1991b](#)

C.D. Parks **A review of the mechanisms of cambering and valley bulging**

A. Forster, M.G. Culshaw, J.C. Cripps, J.A. Little, C.F. Moon (Eds.), Quaternary Engineering Geology, 7 (1991), pp. 373-380

(Geological Society Engineering Geology Special Publication.)

[CrossRefView Record in Scopus](#)

[Perrone et al., 2014](#)

A. Perrone, V. Lapenna, S. Piscitelli **Electrical resistivity tomography technique for landslide investigation: a review**

Earth Sci. Rev., 135 (2014), pp. 65-82

[ArticleDownload PDF](#) [CrossRefView Record in Scopus](#)

[Pook, 2013](#)

G.G. Pook **A Spatial Analysis of Cambering in Jurassic Strata of the Cotswolds and Northamptonshire Ironstone Field**

Unpublished dissertation for MSc in Applied Environmental Geology, Cardiff University (2013)

[Richardson, 1929](#)

L. Richardson **The country around Moreton in Marsh**

Memoir of the Geological Survey of Great Britain, Sheet 217 (1929)

(England and Wales)

[Rodríguez et al., 2014](#)

V. Rodriguez, F. Gutierrez, A.G. Green, D. Carbonel, H. Horstmeyer, C. Schmelzbach **Characterizing sagging and collapse sinkholes in a mantled karst by means of ground penetrating radar (GPR)**

Environ. Eng. Geosci., 20 (2014), pp. 109-132

[CrossRefView Record in Scopus](#)

[Self, 1986](#)

C.A. Self **(for 1985). Two gull caves from the Wiltshire/Avon border**

Proceedings of the University of Bristol Spelaeological Society, 17(1986), pp. 153-174

[View Record in Scopus](#)

[Self, 2008](#)

C.A. Self **Cave passages formed by a newly recognised type of mass movement: a gull tear**

Proceedings of the University of Bristol Spelaeological Society, 24(2008), pp. 101-106

[View Record in Scopus](#)

[Self and Boycott, 2007](#)

C.A. Self, A. Boycott **(for 2006). Landslip caves of the northern Cotswolds**

Proceedings of the University of Bristol Spelaeological Society, 24(2007), pp. 53-70

[Štěpančíková et al., 2011](#)

P. Štěpančíková, J. Dohnal, T. Panek, M. Łoj, V. Smolková, K. Šilhan **The application of electrical resistivity tomography and gravimetric survey as useful tools in an active tectonics study of the Sudetic Marginal Fault (Bohemian Massif, central Europe)**

J. Appl. Geophys., 74 (2011), pp. 69-80

[ArticleDownload PDF](#) [View Record in Scopus](#)

[Suski et al., 2010](#)

B. Suski, G. Brocard, C. Authemayou, B.C. Muralles, C. Teyssier, K. Holliger **Localization and characterization of an active fault in an urbanized area in central Guatemala by means of geoelectrical imaging**

Tectonophysics, 480 (2010), pp. 88-98

[ArticleDownload](#) [PDFView Record in Scopus](#)

[Telford et al., 1990](#)

W.M. Telford, L.P. Geldart, R.E. Sheriff **Applied geophysics**

Cambridge University Press., Cambridge, UK; New York (1990)